# STRUCTURAL STUDIES
# OF MAGNETIC NANOPARTICLES DOPED
# WITH RARE-EARTH ELEMENTS

**T. A. Lastovina[1], A. L. Bugaev[1], S. P. Kubrin[2],**
**E. A. Kudryavtsev[3], and A. V. Soldatov[1]**

UDC 544.178

Magnetic nanoparticles and those doped with rare-earth metal ions having spinel structure were synthesized, possessing the average particles size of 11.3-13.4 nm. According to Mössbauer spectroscopy data it can be concluded that prepared iron oxide nanoparticles are $\gamma$-$Fe_2O_3$. For materials containing rare-earth elements the decrease of octahedral component surface was observed in comparison to non-doped material, what can be explained by $Eu^{3+}$, $Sm^{3+}$ и $Gd^{3+}$ ions occupying the octahedral position.

## INTRODUCTION

Magnetic nanoparticles find their numerous applications in biology and medicine, as a materials for magnetic resonance therapy, hyperthermia, target drug delivery [1-3], and also for development of biosensors [4] and magnetic data recording devices [5]. Due to their high biocompatibility and possibility for natural removal from the body [6] iron oxide nanoparticles play a special role among other magnetic materials for bio-medical applications [7]. In particular, various iron oxides, magnetite ($Fe_3O_4$) and maghemite ($\gamma$-$Fe_2O_3$), are applied for the treatment of oncological diseases [8]. The physical and chemical properties of these nanoparticles to a great extend depend on their size and shape distribution, as well as atomic and electronic structures [9, 10]. It is reported that the highest efficiency in clinical research has been demonstrated by superparamagnetic nanoparticles with average sizes less than 20 nm and with narrow size distribution [11, 12]. It is also known that due to higher magnetic susceptibility magnetite is considered to be more preferable iron oxide phase for medical applications in comparison with maghemite [13]. Therefore, identification of atomic, electronic and magnetic structures of the iron oxide nanoparticles is an important task needed for the optimization of the methods for nanoparticle synthesis for the certain bio-medical requirements.

X-ray diffraction is the most widespread method for studies of crystalline materials. Since both magnetite and maghemite have a cubic spinel-type crystal structure with similar cell parameters [14-16], these iron oxide phases cannot be distinguished by the standard X-ray diffraction technique because the correlation between their diffraction profiles is higher than 99% [17]. Additional information on size and shape of the nanoparticles is possible to obtain from x-ray diffraction data by using pair distribution function approach (PDF) [18].

[1]International Research Center "Smart materials", Southern Federal University, Rostov-on-Don, Russia; lastovina@sfedu.ru. [2]Department of Physics, Southern Federal University, Rostov-on-Don, Russia. [3]Joint Research Center "Diagnostics of structure and properties of nanomaterials", Belgorod National Research University, Russia. Translated from *Zhurnal Strukturnoi Khimii*, Vol. 57, No. 7, pp. 1523-1528, September-October, 2016. Original article submitted December 10, 2015.

In most of the studies, there are some additional methods applied for determination of the iron oxide phase such as X-ray absorption near-edge fine structure (XANES) [19], Raman spectroscopy [20], infra-red Fourier transformed spectroscopy [20-22] and X-ray photoelectron spectroscopy [23, 24]. The number of studies demonstrates the advantages of Mössbauer spectroscopy in distinguishing magnetite and maghemite [25-28].

The aim of the current work was the synthesis and characterization of the structure of the magnetic nanoparticles. The iron oxides were chosen to form the magnetic particles. According to the literature data doping of the magnetic nanoparticles by rare-earth elements ($Sm^{3+}$, $Eu^{3+}$, $Gd^{3+}$) can enhance their magnetic properties and improve their resistivity to oxidation [29]. Therefore, the obtained magnetic nanoparticles were doped by $Sm^{3+}$, $Eu^{3+}$, $Gd^{3+}$ ions during the synthesis.

## EXPERIMENTAL

**Synthesis of magnetic nanoparticles.** Magnetic nanoparticles were synthesized by modified co-precipitation technique. For this purpose hydrazine monohydrate solution (5 ml) in water (100 ml) was prepared in a closed vessel. After stirring during 30 min iron salts $FeCl_2$ (0.002 mol), $FeCl_3$ (0.004 mol) and then, immediately, ammonia solution were added (excess). Solution was heated to 90°C and stirred during 1.5 h. Then, precipitate was separated by the magnet, washed with water and dried in vacuum oven at 60°C. Besides undoped material, also magnetic particles doped with ions of rare-earth elements were prepared. In this case, synthesis was analogies to the one described previously and with the difference of addition of $1.1 \cdot 10^{-4}$ mol of rare-earth element along with iron chloride salts. The quantity of rare-earth precursors was chosen to have moles of rare-earth metal ions from the sum of its moles and moles of obtained magnetite (at 100% yield) equal to 5.2%.

**Characterization.** Powdered samples were investigated by X-ray diffraction in the range of 2θ angles from 25° to 95° on a Rigaku Ultima IV diffractometer ($CuK_{\alpha}$, λ = 0.15406 nm) using 40 kV and 40 mA. The diffraction pattern was recorded with a scanning speed of 0.02° and 2 s exposition time.

Chemical composition of the prepared materials was defined by 2D micro X-ray fluorimeter M4 TORNADO (Bruker).

Microscopic imaging was performed on transmission electron microscope JEM-2100 (JEOL) with accelerating voltage of 200 kV.

Mössbauer spectra of nanopowdered samples were measured by using MS1104Em spectrometer. [57]Co in Cr matrix was used as a source for γ-quants. Model description of the spectra was done by UnivemMS programme. Samples were cooled in refrigerating camera of helium cryostat with CCS-850 closed circulation loop.

## RESULTS DISCUSSION

Diffraction patterns of the obtained materials are shown in Fig. 1. Positions of 2θ maxima evidencing the formation of iron oxide with spinel structure.

The average size of crystallites estimated from Debye–Scherrer [30] equation as well as lattice parameters obtained from Rietveld refinement analysis are given in Table 1.

From the presented data it is clear that doping of the magnetic particles with samarium will not lead to change in average crystallites size in comparison with undoped material. In the same time introduction of gadolinium does not affect significantly the average size while introduction of europium increases the particles average size for 2.1 nm. How it comes from the results of X-ray fluorescence method the doping components are found in iron oxide structure in different quantities (wt.%).

Images taken from transmission electron microscopy (TEM) are presented in Fig. 2. Average particle size according to TEM data is coincide well with average crystallite size calculated from X-ray diffraction data.

Co-precipitation is a most widespread method for the magnetite preparation. It is important to establish an inert atmosphere during the synthesis to prevent oxidation of $Fe^{2+}$ by oxygen and formation of iron(III) oxide. However, number of
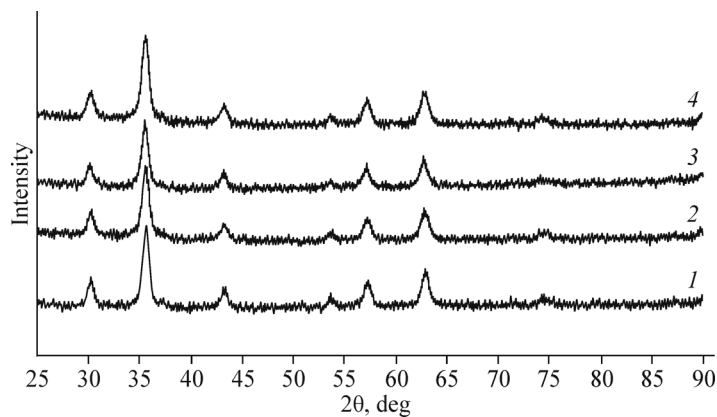
**Fig. 1.** X-ray diffraction patterns of the iron oxide (*1*) and iron oxides doped with $Sm^{3+}$ (*2*), $Gd^{3+}$ (*3*), $Eu^{3+}$ (*4*).

studies points that introduction of hydrazine in to the system allows to conduct the synthesis without blowing through the reaction medium argon or nitrogen. In this case hydrazine plays two-fold activity. From one side, it adsorbs oxygen present

**TABLE 1.** Microstructural Characteristics of the Prepared Magnetic Particles

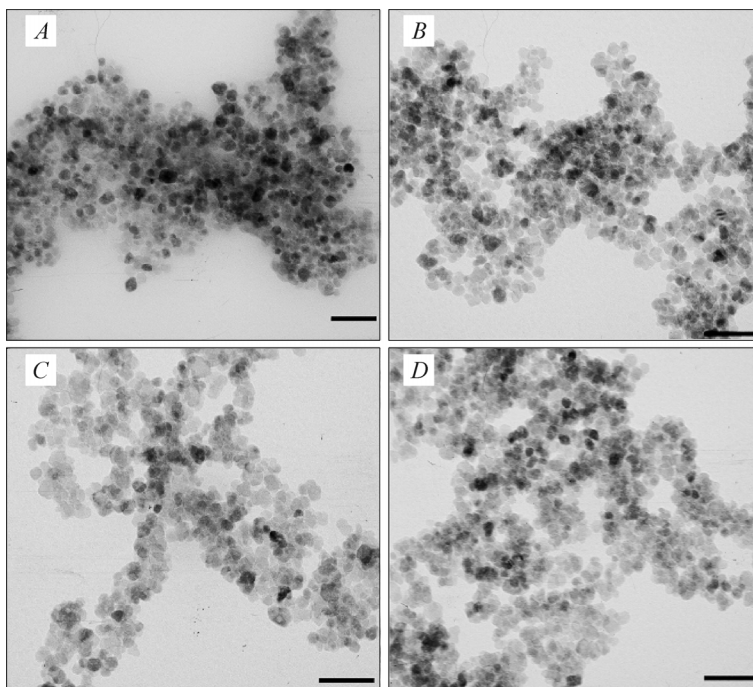| Sample | $D_{av}$, nm (XRD) | Lattice parameter, A | $D$, nm (TEM) | Elements content, wt.% |
|---|---|---|---|---|
| Magnetic particles | 11.3 | 8.3685(14) | 11.5 | – |
| Magnetic particles doped with $Sm^{3+}$ | 11.1 | 8.3628(16) | 11.0 | Fe 94.76  Sm 5.24 |
| Magnetic particles doped with $Gd^{3+}$ | 12.0 | 8.372(4) | 12.1 | Fe 95.81  Gd 4.19 |
| Magnetic particles doped with $Eu^{3+}$ | 13.4 | 8.365(2) | 13.6 | Fe 93.68  Eu 6.32 |



**Fig. 2.** Images obtained by transmission electron microscopy for undoped iron oxide (*A*) and iron oxides doped with $Sm^{3+}$ (*B*), $Gd^{3+}$ (*C*), $Eu^{3+}$ (*D*). The scale bar corresponds to 50 nm.
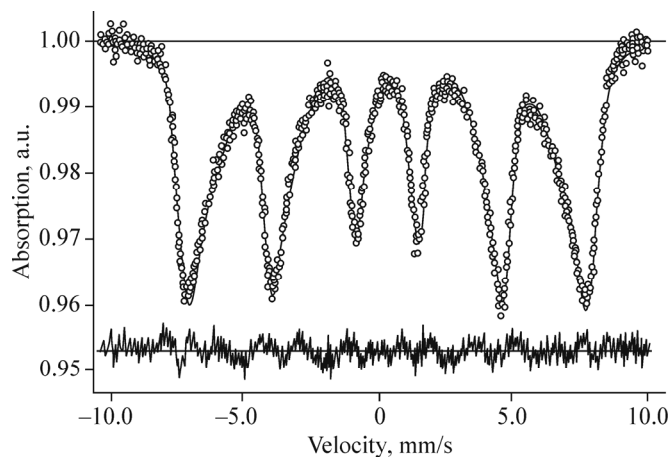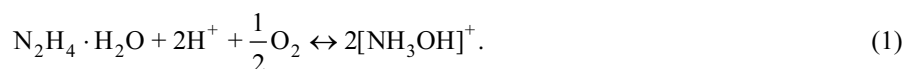
**Fig. 3.** Mössbauer spectrum for undoped iron oxide measured at room temperature.

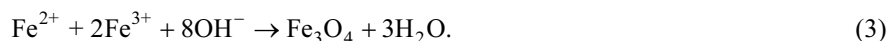in water according to the reaction [31]

$$N_2H_4 \cdot H_2O + 2H^+ + \frac{1}{2}O_2 \leftrightarrow 2[NH_3OH]^+. \tag{1}$$

Apart from this, the formed cation $[NH_3OH]^+$ may react with c $Fe^{2+}$ [32]

$$3Fe^{2+} + [NH_3OH]^+ + 6OH^- \rightarrow Fe_3O_4 + [NH_4]^+ + 3H_2O. \tag{2}$$

At this point, establishment of strong alkaline medium is an important factor [31, 32]. The main reaction remains the same

$$Fe^{2+} + 2Fe^{3+} + 8OH^- \rightarrow Fe_3O_4 + 3H_2O. \tag{3}$$

The next stage was investigation of formed oxides by Mössbauer spectroscopy. Mössbauer spectra of prepared samples measured at room temperature appeared as a poorly resolved Zeeman sextet (Fig. 3).

Observed results indicate a relatively low temperature of magnetic phase transformation. It evidences that temperature of the magnetic phase transition in these samples is rather lower than that in microcrystalline $Fe_3O_4$ or $Fe_2O_3$ materials, the observation is fairly common for the iron oxides nanopowders possessing superferromagnetic properties. Processing of the spectra with poorly resolved spectra Zeeman sextets is difficult, thus, the series of measurements were carried out at 13 K where effective fields on the $^{57}Fe$ cores reached the saturation and Mössbauer spectra are well resolved.

Fig. 4 shows Mössbauer spectra measured at 13 K. Spectrum of each sample presents a superposition of two Zeeman sextets, which parameters listed in Table 2. The both sextets correspond to $Fe^{3+}$ ions wherein the sextet S#1 is corresponded to the tetrahedral arrangement and S#2 to the octahedral one. The presence of $Fe^{3+}$ ions only allows suggesting that investigated samples are not the $Fe_3O_4$ nanopowders. In the same time, the presence of both tetrahedral and octahedral oxygen polyhedrons allows concluding that investigated samples are γ-$Fe_2O_3$.

**TABLE 2.** Parameters of the Mössbauer Spectra for the Iron Oxides Nanopowders

| Sample | $T$, K | Component | δ, mm/s | Δ, mm/s | $H$, kOe | $S$, % | $G$, mm/s | $\chi^2$ |
|---|---|---|---|---|---|---|---|---|
| Magnetic nanoparticles | 13 | S#1 | 0.40 | −0.02 | 513.18 | 61.33 | 0.70 | 2.4 |
|  |  | S#2 | 0.50 | 0.02 | 528.12 | 38.67 | 0.50 |  |
| Magnetic particles doped with $Sm^{3+}$ | 13 | S#1 | 0.41 | −0.02 | 510.49 | 65.90 | 0.68 | 2.4 |
|  |  | S#2 | 0.51 | 0.01 | 527.17 | 34.10 | 0.48 |  |
| Magnetic particles doped with $Gd^{3+}$ | 13 | S#1 | 0.41 | −0.02 | 511.03 | 67.85 | 0.68 | 2.9 |
|  |  | S#2 | 0.51 | 0.01 | 527.70 | 32.15 | 0.45 |  |
| Magnetic particles doped with $Eu^{3+}$ | 13 | S#1 | 0.41 | −0.02 | 510.52 | 66.49 | 0.67 | 3.0 |
|  |  | S#2 | 0.51 | 0.01 | 527.67 | 33.51 | 0.48 |  |
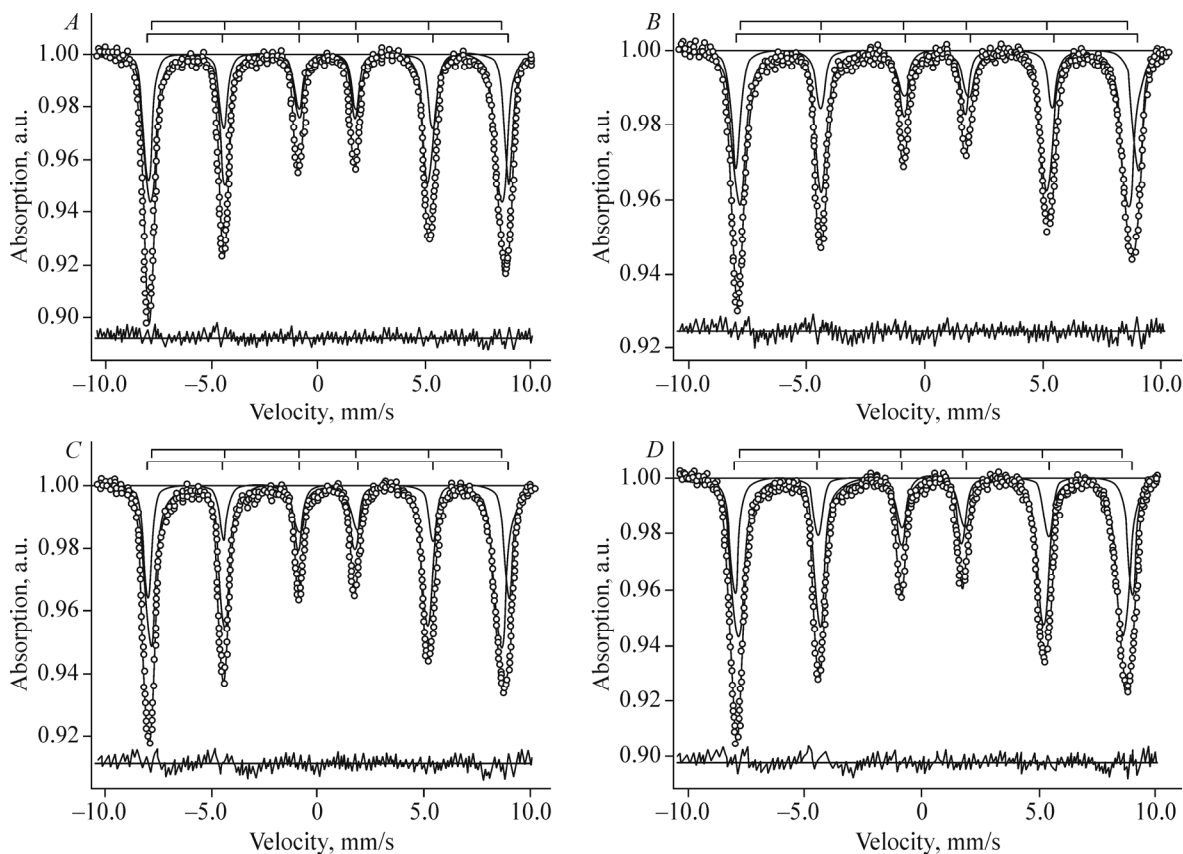
**Fig. 4.** Mössbauer spectra measured at 13 K for (*A*) iron oxide and iron oxides doped with $Sm^{3+}$ (*B*), $Gd^{3+}$ (*C*), $Eu^{3+}$ (*D*).

It should be noted that for the samples containing rare-earth elements there is decrease in area of octahedral component in comparison with undoped materials. Reduction of the S#2 component area can be explained tendency for $Eu^{3+}$, $Sm^{3+}$ and $Gd^{3+}$ ions to occupy the octahedral positions.

In summary, the magnetic nanoparticles with spinel structure were prepared by modified co-precipitation method. Particle size estimated by Scherrer equation coincides well that obtained from transmission electron microscopy data. According to Mössbauer spectra it has been concluded that prepared iron oxide nanoparticles are $\gamma$-$Fe_2O_3$.

## REFERENCES

1. H. Gu, K. Xu, C. Xu, and B. Xu, *Chem. Commun*., No. 9, 941-949 (2006).
2. A. K. Gupta and M. Gupta, *Biomaterials*, **26**, No. 18, 3995-4021 (2005).
3. Q. A. Pankhurst, J. Connolly, S. K. Jones, and J. Dobson, *J. Phys. D: Appl. Phys*., **36**, No. 13, R167-R181 (2003).
4. M. M. Miller, G. A. Prinz, S. F. Cheng, and S. Bounnak, *Appl. Phys. Lett*., **81**, No. 12, 2211-2213 (2002).
5. S. Sun, C. B. Murray, D. Weller, L. Folks, and A. Moser, *Science*, **287**, No. 5460, 1989-1992 (2000).
6. L. Gutierrez, F. J. Lazaro, A. R. Abadia, M. S. Romero, C. Quintana, M. Puerto Morales, C. Patino, and R. Arranz, *J. Inorg. Biochem*., **100**, No. 11, 1790-1799 (2006).
7. S. Laurent, D. Forge, M. Port, A. Roch, C. Robic, L. Vander Elst, and R. N. Muller, *Chem Rev*., **108**, No. 6, 2064-2110 (2008).
8. T. Kikumori, T. Kobayashi, M. Sawaki, and T. Imai, *Breast Cancer Res. Treat*., **113**, No. 3, 435-441 (2009).
9. P. Tartaj, M. D. Morales, S. Veintemillas-Verdaguer, T. Gonzalez-Carreno, and C. J. Serna, *J. Phys. D: Appl. Phys*., **36**, No. 13, R182-R197 (2003).

10. M. P. Morales, S. Veintemillas-Verdaguer, M. I. Montero, C. J. Serna, A. Roig, L. Casas, B. Martínez, and F. Sandiumenge, *Chem. Mater.*, **11**, No. 11, 3058-3064 (1999).

11. K. Woo, J. Hong, S. Choi, H. W. Lee, J. P. Ahn, C. S. Kim, and S. W. Lee, *Chem. Mater.*, **16**, No. 14, 2814-2818 (2004).

12. Y. Zhang, N. Kohler, and M. Q. Zhang, *Biomaterials*, **23**, No. 7, 1553-1561 (2002).

13. B. D. Cullity (ed.), *Introduction to Magnetic Materials*, Addison-Wesley Pub. Co., Reading, MA (1972).

14. M. E. Fleet, *Acta Crystallogr., Sect. B: Struct. Crystallogr. Cryst. Chem.*, **37**, No. 4, 917-920 (1981).

15. V. Rao, A. L. Shashimohan, and A. B. Biswas, *J. Mater. Sci.*, **9**, No. 3, 430-433 (1974).

16. K. Haneda and A. H. Morrish, *J. Phys. Colloq.*, **38**, No. C1, C1-321-C1-323 (1977).

17. W. Kim, C. Y. Suh, S. W. Cho, K. M. Roh, H. Kwon, K. Song, and I. J. Shon, *Talanta*, **94**, 348-352 (2012).

18. V. Petkov, P. D. Cozzoli, R. Buonsanti, R. Cingolani, and Y. Ren, *J. Am. Chem. Soc.*, **131**, No. 40, 14264-14266 (2009).

19. A. Espinosa, A. Serrano, A. Llavona, J. J. de la Morena, M. Abuin, A. Figuerola, T. Pellegrino, J. F. Fernandez, M. Garcia-Hernandez, G. R. Castro, and M. A. Garcia, *Meas. Sci. Technol.*, **23**, No. 1, 015602 (2012).

20. M. M. Can, S. Ozcan, A. Ceylan, and T. Firat, *Mater. Sci. Eng., B*, **172**, No. 1, 72-75 (2010).

21. H. Yan, J. Zhang, C. You, Z. Song, B. Yu, and Y. Shen, *Mater. Chem. Phys.*, **113**, No. 1, 46-52 (2009).

22. Y.-H. Zheng, Y. Cheng, F. Bao, and Y.-S. Wang, *Mater. Res. Bull.*, **41**, No. 3, 525-529 (2006).

23. S. R. Chowdhury, E. K. Yanful, and A. R. Pratt, *Environ. Earth Sci.*, 64, No. 2, 411-423 (2010).

24. C. S. Kuivila, J. B. Butt, and P. C. Stair, *Appl. Surf. Sci.*, **32**, Nos. 1/2, 99-121 (1988).

25. J. L. Dormann, D. Fiorani, R. Cherkaoui, E. Tronc, F. Lucari, F. D'Orazio, L. Spinu, M. Noguès, H. Kachkachi, and J. P. Jolivet, *J. Magn. Magn. Mater.*, **203**, Nos. 1-3, 23-27 (1999).

26. M. Mikhaylova, D. K. Kim, N. Bobrysheva, M. Osmolowsky, V. Semenov, T. Tsakalakos, and M. Muhammed, *Langmuir*, **20**, No. 6, 2472-2477 (2004).

27. J. Santoyo Salazar, L. Perez, O. de Abril, L. Truong Phuoc, D. Ihiawakrim, M. Vazquez, J.-M. Greneche, S. Begin-Colin, and G. Pourroy, *Chem. Mater.*, **23**, No. 6, 1379-1386 (2011).

28. E. Tronc, A. Ezzir, R. Cherkaoui, C. Chanéac, M. Noguès, H. Kachkachi, D. Fiorani, A. M. Testa, J. M. Grenèche, and J. P. Jolivet, *J. Magn. Magn. Mater.*, **221**, Nos. 1/2, 63-79 (2000).

29. W. Huan, C. Cheng, Y. Yang, H. Yuan, and Y. Li, *J. Nanosci. Nanotechnol.*, **12**, No. 6, 4621-4634 (2012).

30. P. Scherrer, *Nachr. Ges. Wiss. Goettingen, Math.-Phys. Kl.*, **2**, 98-100 (1918).

31. D. Gingasu, I. Mindru, L. A. Patron, J. M. Calderon-Moreno, L. Diamandescu, F. Tuna, and T. Popescu, *Dig. J. Nanomater. Biostruct. (DJNB)*, **6**, No. 3, 1065-1072 (2011).

32. R. Y. Hong, J. H. Li, H. Z. Li, J. Ding, Y. Zheng, and D. G. Wei, *J. Magn. Magn. Mater.*, **320**, No. 9, 1605-1614 (2008).